2023 IEEE Symposium Series on Computational Intelligence (SSCI)
Mexico City, Mexico. December 5-8, 2023

Integrated Connectivity-based Stacking Ensemble Learning with GCNNs for EEG Representation

1st Abdullah Almohammadi
CIBCI Lab, Australian Artificial Intelligence Institute, Faculty of Engineering and Information Technology, University of Technology Sydney
Abdullah.Almohammadi@student.uts.edu.au

2nd Yu-Kai Wang
CIBCI Lab, Australian Artificial Intelligence Institute, Faculty of Engineering and Information Technology, University of Technology Sydney
YuKai.Wang@uts.edu.au

***Abstract*—This study proposes a novel approach that combines stacking ensemble learning with Graph Convolutional Neural Networks (GCNNs) to enhance the classification accuracy of Motor Imagery (MI) tasks in supporting individuals with injuries or impairments, enabling more effective rehabilitation and assistance. The method integrates both structural and functional connectivity information to leverage the benefits of GCNNs and ensemble learning techniques. The BCI Competition IV-2a dataset is used for evaluation. The approach employs a stacked ensemble model consisting of nine baseline models and six combining meta-models, including Logistic Regression, Neural Networks, Support Vector Machines, Random Forest, K-Nearest Neighbor, and Gradient Boosting Machine. By leveraging information from both structural and functional connectivity, the GCNNs extract meaningful features from MI data, leading to improved classification accuracy. The stacking ensemble learning technique combines multiple GCNN models trained on different connectivity aspects, resulting in a robust and accurate classifier. The fusion of structural connectivity (ADJ-CNNM) capturing anatomical connections and functional connectivity (PLV-CNNM) measuring brain activity synchronization enables a comprehensive analysis of MI data. The proposed approach effectively captures both local and global connectivity patterns, addressing the challenges associated with MI data analysis. By considering both types of connectivity, a holistic understanding of the dynamics of the underlying brain network during MI tasks is achieved. Experimental results demonstrate the effectiveness of the proposed approach, achieving an accuracy of 86.23% with K-Nearest Neighbor as the meta-model. Comparisons with state-of-the-art and baseline methods on the same dataset validate the approach's superiority, emphasizing the importance of GCNNs and stacking ensemble learning for accurate MI task classification.**

***Index Terms*—Motor Imagery(MI), Stacking Ensemble Learning, GCNNs, Structural Connectivity, Functional Connectivity**

I. Introduction

Brain-computer interfaces (BCIs) aim to restore or replace functional abilities in individuals with neuromuscular disorders, such as spinal cord injury and stroke rehabilitation [1]. Electroencephalographic (EEG) signals, which capture cortical electrical activity, have gained popularity in BCI development due to their convenience and scalp recording. However, the focus on subject-dependent scenarios in most studies limits the scalability and applicability of BCIs due to inherent variations in EEG signals [2]. Conventional MI-EEG analysis relies on handcrafted features and machine learning algorithms, such as power spectral density (PSD). Recent advancements in deep learning have shown promise in effectively learning information across subjects [3]. In MI-EEG classification, various methods have emerged to enhance performance. Common Spatial Pattern (CSP) and Filter Bank CSP (FBCSP) are widely used techniques that maximize power differences between MI classes [4]. Deep learning models, such as Convolutional Neural Networks (CNNs) with crop training techniques and Recurrent Neural Networks (RNNs), capture temporal information in MI classification [5]. Graph Neural Networks (GNNs) have also gained significance in analyzing brain dynamics and connectivity [6]. Additionally, ensemble learning techniques explored in MI-EEG classification consistently prove effective in improving reliability and accuracy by mitigating variability and noise [7]–[9].

This study addresses limitations in existing studies while introducing novel contributions:

1) **Enhanced Subject Independence with ADJ-CNNM**: Subject-specific scenarios, which limit BCI scalability, are addressed by the ADJ-CNNM model. Spatial information is efficiently captured, and EEG graphs are constructed based on precise spatial EEG electrode data, enhancing subject independence. This expansion of BCI applicability mitigates subject-dependent limitations.
2) **Innovative Integration of GCNNs**: Complex EEG patterns often go uncaptured in traditional MI-EEG analysis. GCNNs are introduced in this study, offering a comprehensive capture of both local and global connectivity patterns in EEG data. This innovative integration enhances the effectiveness of MI-EEG classification by enabling the extraction of richer EEG information.
3) **Diverse Analysis with Multiple Connectivity Types**: The limitation of model diversity is addressed by incorporating both structural and functional connectivity with multiple frequency band variations in the analysis. This comprehensive analysis enables a holistic understanding of brain network dynamics during MI tasks.
4) **Optimized Ensemble Learning**: Untapped potential for enhancing reliability and accuracy lies in ensemble techniques in MI-EEG classification. Stacking ensemble learning is employed in this study, combining diverse GCNN models to capture complementary information. This approach significantly improves clas-

sification accuracy, demonstrating the method's effectiveness.

5) **Validation of Superiority**: Validation against state-of-the-art and baseline techniques using the same dataset underscores the superiority of the proposed approach in the field of MI-EEG classification.

II. Methodology

This work presents a proposed method that employs stacking ensemble learning with Graph Convolutional Neural Networks (GCNNs) to leverage structural and functional connectivity for improved classification of MI tasks, as shown in Fig. 1. The objective of this approach is to enhance the accuracy and performance of MI classification by integrating the benefits of GCNNs and ensemble learning techniques. The study utilized the BCI Competition IV-2a dataset [10], a widely recognized benchmark dataset for EEG analysis. It consisted of 22 EEG signals from nine healthy individuals, collected in two sessions on different days, where participants mentally simulated movements of their left hand, right hand, feet, and tongue during 288 four-second trials per session.

A. Structural Connectivity-Based Graph Representation

The structural connectivity-based graph methodology is depicted in Fig.1a. Initially, the EEG signals are transformed into a graph representation through adjacency matrices, followed by the utilization of a neural network to process the encoded signals. This end-to-end framework enables training through conventional back-propagation methods.

The ADJ-CNNM model is a convolutional neural network that leverages EEG node graph representations to efficiently capture spatial information. By utilizing this approach, the challenge of subject-independence in MI-EEG Classification can be effectively tackled. An EEG graph is initially constructed based on the precise spatial information of the EEG electrodes, representing the interconnections between them. Unlike previous spatial filtering methods that depend on specific subjects or tasks, the proposed graph embedding technique offers greater flexibility and reliability for new subjects.

1) EEG Node Connection Representations: The length of MI tasks in the BCI Competition IV-2a dataset is of research interest, measured in T-seconds. Each of the n EEG nodes is accompanied by an associated sensor recording sequence. $r_i \in [1, n] = [\text{sig}_1^i, \text{sig}_2^i, \text{sig}_3^i, \ldots, \text{sig}_m^i] \in \mathbb{R}^m$ via $m = T * f$ time instances, where f represents the sampling frequency rate and sig_t^i corresponds to the reading taken by the ith EEG sensor at a given time instance t. Therefore, the EEG signal features of trial t is a 2D tensor $X_T = [\text{sig}_1; \text{sig}_2, \ldots, \text{sig}_n] \in \mathbb{R}^{n*m}$ where the EEG nodes are represented by one dimension, and the time series is represented by the second dimension. When examining EEG nodes, it is crucial to consider their associations with neighboring nodes. The traditional approach limits each EEG node to a maximum of two neighbors in the X_T node dimension. However, in reality, EEG nodes typically have numerous neighbors that capture signals from specific brain regions. To accurately capture the spatial relationships between EEG nodes, an undirected spatial graph was constructed, denoted as $G = (V, E)$, where V represents the set of vertices, $V = \text{sig}^i | i \in [1, n]$, encompassing all the nodes.

This graph representation is derived from the adjacency matrix of the EEG nodes, which captures their spatial associations. By adopting this graph representation, EEG signals become more effective in representing distinct brain regions and mitigating the influence of noise by grouping neighboring nodes to represent the core node. Consequently, this methodology allows each EEG node to rely on the support of its neighboring nodes, promoting robustness in EEG data representation even in the presence of missing values.

2) Adjacency Matrix Graph (Adj-Graph): The arrangement of 22 EEG nodes in Fig. 1a showcases their neighboring nodes situated in different directions, such as up, down, left, right, up-left, up-right, down-left, and down-right. For example, node sig^{10} has eight neighboring nodes in this configuration, namely $sig^{16}, sig^4, sig^{11}, sig^9, sig^{17}, sig^{15}, sig^5$, and sig^3. In order to establish connections between naturally adjacent EEG nodes, a set of edges was created, denoted as $E_v = sig^i sig^j | (i, j) \in H$, where H represents the set of all adjacent EEG nodes. It should be noted that each node is considered to be connected to itself. The adjacency matrix of the adj-Graph is a square matrix of size $|V| \times |V|$, where each entry is a binary value indicating whether two EEG nodes are adjacent or not.

The spectral graph theory [11] was utilized to normalize the adjacency matrix.

Following the application of Adj-Graph embedding to EEG signals, a convolutional neural network (CNN) was employed to encode and extract temporal features for classifying MI data. While deep networks demonstrate learning capabilities, they may not be the optimal choice for EEG analysis [12]. The model configuration consisted of a single CNN layer and a single max pooling layer. To consider all EEG nodes simultaneously, the CNN kernel height was set to 22, corresponding to the number of EEG nodes in the dataset. Increasing the kernel width to 45 was based on the need to capture long-term temporal dynamics more effectively. This choice was empirically determined through experimentation to achieve better model performance. Moreover, 64 CNN filters were empirically chosen to reveal spatio-temporal information across multiple EEG nodes effectively. The selection of this hyperparameter was based on experiments that demonstrated its effectiveness in capturing relevant information in the EEG signals. Rectified Linear Units (ReLU) were employed as the activation function in the convolutional process. Spatial resolution reduction was achieved by setting the CNN's stride size to (2,2). A max-pooling layer was utilized to extract significant features and reduce dimensionality. Furthermore, a dropout regularization layer with a rate of 25% was applied to prevent overfitting and enhance model generalization. The specific rate of 25% was chosen based on experiments that demonstrated a good balance between preventing overfitting and maintaining model performance. For the final layer, a

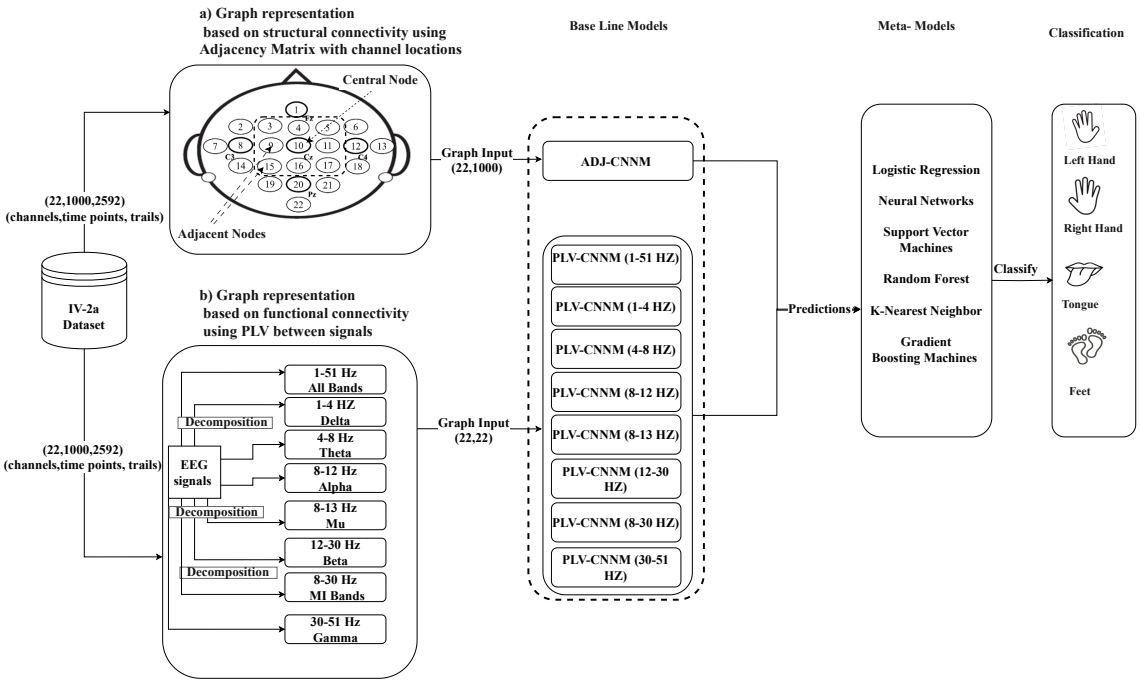

Fig. 1: Stacking Ensemble Learning with GCNNs Incorporating Structural and Functional Connectivity. A Stacked Model with 9 Baseline Models and 6 Combining Meta-Models.

dense layer with a softmax classifier was used to predict the probability distribution of the four classes.

B. Functional Connectivity-Based Graph Representation

The functional connectivity-based graph methodology, as depicted in Fig.1b, involves several essential steps to analyze EEG signals effectively. Firstly, the EEG signals are decomposed to extract specific frequency bands, including δ, θ, α, μ, β, γ and (1-51 Hz), covering a broad range of brain activity. Next, these EEG signals are transformed into a graph representation using Phase Locking Value (PLV), which captures the synchronization between different brain regions. This graph representation allows for the characterization of functional connectivity patterns across the brain. Subsequently, the encoded EEG signals are fed into a neural network. This comprehensive framework represents an end-to-end model, suitable to training through standard back-propagation methods.

1) EEG-channel Connection Representations : Phase synchronization events are frequently observed in EEG data and have found widespread application in studies related to motion imaging and BCIs [13]. Compared to other techniques for evaluating phase synchronization between signals, they are often preferred. PLV [14], [15] is a measure used to quantify the degree of synchronization between two EEG channels, indicating the extent to which their signals are correlated over time. One commonly employed method for representing EEG channel connections based on PLV is the creation of a connectivity matrix, also referred to as a functional connectivity network. In this matrix, each row and column corresponds to a distinct EEG channel, and the value in each cell represents the PLV between the corresponding pair of channels. PLV serves as an indicator of the average phase difference between any two signals, allowing for the differentiation of the phase component from the amplitude component of EEG signals. The formula that defines PLV is provided in [16], and it can be represented as follows:

$$PLV(t) = \frac{1}{N}\left|\sum_{1}^{N} exp(i(\triangle\varphi_n(t)))\right| \tag{1}$$

The phase difference between the signals recorded by electrode x and electrode y at time t is given by $\triangle\varphi_n(t) = \varphi_x(t) - \varphi_y(t)$ The length of the time series is represented by N. Each EEG channel is depicted as a node in the graph, and the edges of the graph represent the PLV values between the channels. Therefore, the graph is constructed based on the PLV connectivity among the different nodes. Analyzing the connectivity patterns between different brain regions and investigating the functional interactions between them through this graph provides valuable insights into the network properties of the brain.

2) Phase Locking Value Graph (PLV-Graph): PLV measures the consistency of phase differences between signals and enables the construction of a graph representing EEG signal connectivity. Each channel is a node, and edges indicate functional connectivity strength. The PLV-CNNM graph follows three steps: (A) Calculate PLV values between the 22 EEG channels. (B) Represent EEG channels as nodes, incorporating significant PLV connections as edges. (C) Assign weights to edges based on PLV strength. This undirected graph identifies non-directional connectivity patterns. Decomposing EEG signals extracts desired frequency bands: δ (1-4 Hz), θ (4-8 Hz), α (8-12 Hz), μ (8-13 Hz), β (12-30

Hz), and γ (30+ Hz). PLV values are computed between each pair of EEG channels using Equation 1.

N represents the number of signals, i is the imaginary unit, and $\triangle\varphi_n(t) = \varphi_x(t) - \varphi_y(t)$ signifies phase difference between signals at time t. PLV ranges from 0 to 1, indicating no synchronization and perfect synchronization. Connections derived from PLV form a graph illustrating connectivity among brain regions at varying frequencies. Each EEG channel is a node, and connections are edges. This approach reveals brain network organization and information flow patterns. The PLV graph identifies network hubs, modules, and changes in properties. It investigates the relationship between EEG connectivity and cognitive processes like MI tasks.

The PLV-CNNM architecture includes two CNN layers with a kernel size of (3, 3) to extract complex time-frequency-domain features from the EEG data. A max-pooling layer (2, 2) to reduce spatial resolution and computational complexity while retaining vital information, and a 25% dropout regularization layer to prevent overfitting. The choice of 32 and 64 filters in the convolutional layers reflects the need to capture progressively complex patterns in the EEG data. The initial 32 filters focus on extracting lower-level features, while the subsequent 64 filters operate at a higher level to capture more abstract representations. ReLU activation is used. The final dense layer employs softmax classification for generating a probability distribution across four classes.

C. stacking Ensemble Learning with GCNNs

The concept of stacking, also known as meta-learning, is employed to merge the outcomes of multiple classification models or base models in order to enhance performance [17]. By utilizing an additional learning algorithm called the level-l model or meta-model, stacking aims to identify reliable classifiers. The meta-model takes input in the form of predictions made by the baseline models, referred to as level-0 models. These level-0 models assign scores to each potential class, and subsequently, the outputs of the level-0 models are fed into the level-1 models, which combine them to generate the final prediction.

This study employs a novel approach integrating stacking ensemble learning with GCNNs to analyze MI data. This approach incorporates both structural and functional connectivity, as illustrated in Fig. 1. The Stacked Model consists of Nine Baseline Models and Six Combining Meta-Models, including Logistic Regression, Neural Networks, Support Vector Machines, Random Forest, K-Nearest Neighbor, and Gradient Boosting Machine. These meta-models were chosen to ensure a diverse set of learning strategies for combining outputs from the base models in the stacking ensemble approach. These meta-models have demonstrated their effectiveness in handling diverse input sources and have a track record of success in improving classification performance when used as meta-models. Importantly, they are well-suited for the ensemble approach in this study, which combines information from both structural and functional connectivity. By combining information from both structural and functional connectivity, the approach utilizes GCNNs to extract meaningful features from MI data, ultimately leading to an improvement in classification accuracy. The stacking ensemble learning technique combines multiple GCNN models trained on different aspects of connectivity, resulting in a more robust and accurate classifier for MI tasks. The primary focus lies in the fusion of structural connectivity (ADJ-CNNM), capturing anatomical connections, and functional connectivity (PLV-CNNM) along with its variations, measuring brain activity synchronization. This fusion enables a comprehensive analysis of MI data. By leveraging GCNNs and stacking ensemble learning, this approach effectively captures both local and global connectivity patterns, thereby addressing the challenges associated with analyzing MI data. The integration of structural and functional connectivity information within the GCNN-based ensemble model provides a holistic understanding of the dynamics of the underlying brain network during MI tasks.

III. Results & Discussion

Table. I presents various combinations of stacking ensemble learning, including baseline models and meta-models, which were evaluated to analyze the effectiveness of stacking ensemble learning in analyzing MI tasks. These combinations, incorporating GCNNs, play an integral role in the stacking ensemble learning approach applied to the analysis process. The utilization of stacking ensemble learning enhances classification performance by leveraging the combined predictive power of multiple models.

The stacking ensemble approach in this study incorporates both structural and functional connectivity measures for analyzing motor imagery tasks. ADJ-CNNM focuses on structural connectivity, representing the physical connections between different brain regions. On the other hand, PLV-CNNM (1-51 Hz) captures functional connectivity, which reflects the synchronization of neural activity between brain regions.

By combining these two measures, the model benefits from the complementary information provided by both structural and functional connectivity. Structural connectivity reveals the underlying anatomical framework of the brain, while functional connectivity highlights the dynamic interactions between brain regions during motor imagery tasks. This integration allows the model to obtain a more comprehensive understanding of the brain's network organization and its relevance to motor imagery processes.

Moreover, PLV-CNNM (1-51 Hz) covers a broad frequency range, encompassing various neural oscillations. This wide range enables the model to capture diverse functional connectivity patterns associated with different frequency bands, potentially capturing distinct aspects of motor imagery processes. The synergy between structural and functional connectivity information allows the stacking ensemble approach to improve the classification performance compared to using only one type of connectivity measure. By leveraging both modalities, the model gains a more holistic view of the brain's functional organization during motor imagery

TABLE I: Results of Stacking Ensemble Learning combinations based on 9-fold cross-validation for 10 runs.

Base Line Models	Meta Models	
	Model	**Mean ± Stdev**
ADJ-CNNM	None	72.57% ± 0.045
PLV-CNNM (1-51)	None	75.10% ± 0.018
ADJ-CNNM + PLV-CNNM (1-51)	NN	85.23% ± 0.0208
	SVM	85.30% ± 0.0188
	LR	85.18% ± 0.0209
	RF	84.73% ± 0.0179
	KNN	84.93% ± 0.0185
	GBT	85.04% ± 0.0177
ADJ-CNNM + PLV-CNNM (8-30)	NN	85.18% ± 0.0219
ADJ-CNNM + PLV-CNNM (1-51) + PLV-CNNM (8-30)	NN	85.29% ± 0.0222
ADJ-CNNM + PLV-CNNM (8-12) + PLV-CNNM (8-13) + PLV-CNNM (12-30)	NN	85.20% ± 0.0297
ADJ-CNNM + PLV-CNNM (1-51) + PLV-CNNM (8-12) + PLV-CNNM (12-30)	NN	85.42% ± 0.0210
ADJ-CNNM + PLV-CNNM (1-51) + PLV-CNNM (8-12) + PLV-CNNM (8-13)	NN	85.09% ± 0.0219
ADJ-CNNM + PLV-CNNM (8-12) + PLV-CNNM (12-30)	NN	85.01% ± 0.0167
	SVM	84.89% ± 0.0161
	LR	85.04% ± 0.0174
	RF	84.99% ± 0.0165
	KNN	**86.23%** ± 0.0155
	GBT	85.16% ± 0.0153

tasks, resulting in more accurate predictions and a deeper understanding of the underlying neural mechanisms.

Furthermore, the baseline models, ADJ-CNNM and PLV-CNNM (1-51 Hz), achieve accuracies of 72.57% and 75.10%, respectively. When ADJ-CNNM and PLV-CNNM (1-51 Hz) are combined with different meta-models, the ensemble models show remarkable accuracy increments. The NN meta-model achieves an accuracy of 85.23%, indicating an increment of 12.66% compared to the ADJ-CNNM baseline accuracy. Similarly, the SVM meta-model achieves an accuracy of 85.30%, representing an increment of 12.73%. The LR meta-model achieves an accuracy of 85.18%, reflecting an increment of 12.61%. The RF meta-model achieves an accuracy of 84.73%, with an increment of 12.16%. The KNN meta-model achieves an accuracy of 84.93%, showing an increment of 12.36%. Finally, the GBT meta-model achieves an accuracy of 85.04%, with a noticeable improvement of 12.47%.

When considering the PLV-CNNM (1-51 Hz) baseline accuracy, the NN meta-model achieves an accuracy of 85.23%, indicating an increment of 10.13%. Similarly, the SVM meta-model achieves an accuracy of 85.30%, representing an increment of 10.20%. The LR meta-model achieves an accuracy of 85.18%, reflecting an increment of 10.08%. The RF meta-model achieves an accuracy of 84.73%, with an increment of 9.63%. The KNN meta-model achieves an accuracy of 84.93%, showing an increment of 9.83%. Finally, the GBT meta-model achieves an accuracy of 85.04%, with an increment of 9.94%. These results underscore the effectiveness of stacking ensemble learning in significantly enhancing the classification performance for MI tasks. The combinations of ADJ-CNNM and PLV-CNNM (1-51 Hz) with different meta-models achieve substantial accuracy increments, ranging from 9.63% to 12.73%. This emphasizes the potential of ensemble learning techniques in effectively leveraging the strengths of multiple models to achieve improved and robust classifications.

An alternative combination, ADJ-CNNM and PLV-CNNM (8-30 Hz), targets the relevant α and β bands for MI data, achieving an accuracy of 85.18%. To capture functional connectivity across different frequency ranges, ADJ-CNNM, PLV-CNNM (1-51 Hz), and PLV-CNNM (8-30 Hz) extend the previous combination by including an additional PLV-CNNM feature extracted from the 8-30 Hz range, resulting in an accuracy of 85.29%.

Specializing in α, β and μ the combination of ADJ-CNNM, PLV-CNNM (8-12 Hz), PLV-CNNM (8-13 Hz), and PLV-CNNM (12-30 Hz) achieves an accuracy of 85.20%. A broader range of neural dynamics associated with MI tasks is captured by combining ADJ-CNNM, PLV-CNNM (1-51 Hz), PLV-CNNM (8-12 Hz), and PLV-CNNM (12-30 Hz), resulting in an accuracy of 85.42%.

Additionally, the combination of ADJ-CNNM, PLV-CNNM (1-51 Hz), PLV-CNNM (8-12 Hz), PLV-CNNM (8-13 Hz), and PLV-CNNM (12-30 Hz) encompasses a diverse set of features and achieves an accuracy of 85.09%.

The most discriminative features for MI classification are captured by the combination ADJ-CNNM + PLV-CNNM (8-12 Hz) + PLV-CNNM (12-30 Hz), focusing on the crucial α and β frequency ranges. This combination significantly reduces noise, leading to improved accuracy at 86.23% with KNN as the meta-model, surpassing other models and confirming its ability to capture motor-related neural dynamics in MI data.

To provide context, a comparison with other studies using the same IV-2a dataset was conducted and presented in Table II, affirming the significance of these α and β frequency ranges in MI data analysis and supporting the superiority of this approach.

The study's approach, combining ADJ-CNNM and PLV-CNNM (8-12 Hz) + PLV-CNNM (12-30 Hz) with stacking ensemble learning, successfully captures key discriminatory features, enhances classification accuracy, and provides insights into motor-related neural dynamics. Furthermore, the results and discussions underscore the importance of specific frequency ranges and the effectiveness of stacking ensemble learning. The study confirms that ensemble learning techniques, including stacking ensemble learning, play a crucial role in addressing the inherent variability in EEG signals. By combining the predictions of multiple models, the study demonstrates that ensemble methods effectively mitigate the impact of noise and individual model biases, resulting in significantly improved robustness and accuracy in MI-EEG

TABLE II: An Evaluation of Proposed Methods against State-of-the-Art and Baseline Models on the IV-2a Dataset.

Comparison Model	Mean	Stdev
EEGNet [5]	51.31%	0.051
CTCNN [12]	47.67%	0.150
FBCSP [4]	35.69%	0.083
CNN	47.20%	0.047
RNN	35.48%	0.022
CRAM [18]	59.10%	0.108
NG-RAM [19]	60.11%	0.099
DG-RAM [19]	59.64%	0.097
SG-RAM [19]	59.00%	0.101
T-WaveNet-Haar [20]	43.12%	NA
T-WaveNet (without feature fusion) [20]	61.03%	NA
T-WaveNet [20]	63.01%	NA
Stack Ensemble Methods		
LDA (Linear DA) [7]	62.00%	0.18
SLDA (Stacked Linear DA) [7]	66.00%	0.19
SLD (SVM-LDA-Decision Tree) [8]	77.08%	NA
Ensemble-CNN [9]	64.16%	NA
(ADJ-CNNM + PLV-CNNM (8-12 Hz) + PLV-CNNM (12-30 Hz))	**86.23%**	0.0155

classification.

IV. Conclusion

This study has introduced several contributions to the field of MI. By combining stacking ensemble learning with GCNNs, the study has significantly enhanced the accuracy of MI task classification, promising substantial support for individuals with injuries or impairments in their rehabilitation and assistance needs. The introduction of the ADJ-CNNM model has addressed subject-specific scenarios, enhancing subject independence and expanding the applicability of BCIs. Additionally, the innovative integration of GCNNs has allowed for the comprehensive capture of both local and global connectivity patterns in EEG data, extracting richer information for MI classification. Incorporating multiple connectivity types, including structural and functional connectivity with various frequency band variations, has further diversified the model's analysis capabilities. Furthermore, the study has optimized ensemble learning techniques, specifically employing stacking ensemble learning, to combine diverse GCNN models, thus improving classification accuracy significantly. This approach underscores the effectiveness of ensemble techniques in MI classification. The validation against state-of-the-art and baseline techniques using the same dataset has highlighted the superiority of the proposed approach in the field of MI classification. These contributions collectively emphasize the potential of GCNNs and stacking ensemble learning to address the challenges associated with MI classification. Future research endeavors should build upon these findings, exploring more advanced meta-models, investigating additional features, and assessing the model's performance with larger and more diverse datasets.

References

[1] N. D. López, E. Monge Pereira, E. J. Centeno, and J. C. Miangolarra Page, "Motor imagery as a complementary technique for functional recovery after stroke: a systematic review," *Topics in Stroke Rehabilitation*, vol. 26, no. 8, pp. 576–587, 2019.

[2] H.-I. Suk and S.-W. Lee, "A novel bayesian framework for discriminative feature extraction in brain-computer interfaces," *IEEE Transactions on Pattern Analysis and Machine Intelligence*, vol. 35, no. 2, pp. 286–299, 2012.

[3] A. Essa and H. Kotte, "Brain signals analysis based deep learning methods: Recent advances in the study of non-invasive brain signals," *arXiv preprint arXiv:2201.04229*, 2021.

[4] K. K. Ang, Z. Y. Chin, H. Zhang, and C. Guan, "Filter bank common spatial pattern (fbcsp) in brain-computer interface," in *2008 IEEE international joint conference on neural networks (IEEE world congress on computational intelligence)*. IEEE, 2008, pp. 2390–2397.

[5] V. J. Lawhern, A. J. Solon, N. R. Waytowich, S. M. Gordon, C. P. Hung, and B. J. Lance, "Eegnet: a compact convolutional neural network for eeg-based brain–computer interfaces," *Journal of neural engineering*, vol. 15, no. 5, p. 056013, 2018.

[6] L. Santamaria and C. James, "Use of graph metrics to classify motor imagery based bci," in *2016 International Conference for Students on Applied Engineering (ICSAE)*. IEEE, 2016, pp. 469–474.

[7] L. F. Nicolas-Alonso, R. Corralejo, J. Gómez-Pilar, D. Álvarez, and R. Hornero, "Ensemble learning for classification of motor imagery tasks in multiclass brain computer interfaces," in *2014 6th Computer Science and Electronic Engineering Conference (CEEC)*. IEEE, 2014, pp. 79–84.

[8] M. Rahimi, A. Zarei, E. Nazerfard, and M. H. Moradi, "Ensemble methods combination for motor imagery tasks in brain computer interface," in *2016 23rd Iranian Conference on Biomedical Engineering and 2016 1st International Iranian Conference on Biomedical Engineering (ICBME)*. IEEE, 2016, pp. 336–340.

[9] I. Dolzhikova, B. Abibullaev, R. Sameni, and A. Zollanvari, "An ensemble cnn for subject-independent classification of motor imagery-based eeg," in *2021 43rd Annual International Conference of the IEEE Engineering in Medicine & Biology Society (EMBC)*. IEEE, 2021, pp. 319–324.

[10] C. Brunner, R. Leeb, G. Müller-Putz, A. Schlögl, and G. Pfurtscheller, "Bci competition 2008–graz data set a," *Institute for Knowledge Discovery (Laboratory of Brain-Computer Interfaces), Graz University of Technology*, vol. 16, pp. 1–6, 2008.

[11] T. N. Kipf and M. Welling, "Semi-supervised classification with graph convolutional networks," *arXiv preprint arXiv:1609.02907*, 2016.

[12] R. T. Schirrmeister, J. T. Springenberg, L. D. J. Fiederer, M. Glasstetter, K. Eggensperger, M. Tangermann, F. Hutter, W. Burgard, and T. Ball, "Deep learning with convolutional neural networks for eeg decoding and visualization," *Human brain mapping*, vol. 38, no. 11, pp. 5391–5420, 2017.

[13] J. R. C. Piqueira, "Network of phase-locking oscillators and a possible model for neural synchronization," *Communications in Nonlinear Science and Numerical Simulation*, vol. 16, no. 9, pp. 3844–3854, 2011.

[14] T. R. Goldstein, J. A. Bridge, and D. A. Brent, "Sleep disturbance preceding completed suicide in adolescents." *Journal of consulting and clinical psychology*, vol. 76, no. 1, p. 84, 2008.

[15] X. Gao, H. Cao, D. Ming, H. Qi, X. Wang, X. Wang, R. Chen, and P. Zhou, "Analysis of eeg activity in response to binaural beats with different frequencies," *International Journal of Psychophysiology*, vol. 94, no. 3, pp. 399–406, 2014.

[16] W. Yi, S. Qiu, K. Wang, H. Qi, L. Zhang, P. Zhou, F. He, and D. Ming, "Evaluation of eeg oscillatory patterns and cognitive process during simple and compound limb motor imagery," *PloS one*, vol. 9, no. 12, p. e114853, 2014.

[17] S. Parui, D. Basu, U. Ghosh, and R. Datta, "A brain to uav communication model using stacked ensemble csp algorithm based on motor imagery eeg signal," in *ICC 2022-IEEE International Conference on Communications*. IEEE, 2022, pp. 1–6.

[18] D. Zhang, L. Yao, K. Chen, and J. Monaghan, "A convolutional recurrent attention model for subject-independent eeg signal analysis," *IEEE Signal Processing Letters*, vol. 26, no. 5, pp. 715–719, 2019.

[19] D. Zhang, K. Chen, D. Jian, and L. Yao, "Motor imagery classification via temporal attention cues of graph embedded eeg signals," *IEEE journal of biomedical and health informatics*, vol. 24, no. 9, pp. 2570–2579, 2020.

[20] L. Minhao, A. Zeng, L. Qiuxia, R. Gao, M. Li, J. Qin, and Q. Xu, "T-wavenet: A tree-structured wavelet neural network for time series signal analysis," in *International Conference on Learning Representations*, 2021.